Analysis of sediment transport in the Mekong using the lumped BQART model

MSc thesis

Vivianne in 't Veld

First supervisor: dr. Frances Dunn

Second supervisor: dr. Rens van Beek

Universiteit Utrecht

Abstract

Decreasing sediment concentrations in rivers have led to a decrease in deposition in delta regions worldwide. This has led to an increased flood risk in coastal zones with large potential damages. This decrease in sediment load has been mainly attributed to the construction of dams and reservoirs. Predicting the amount of sediment in a river is vital in order to propose measures to resolve this problem, but discrete models are expensive, have a large computation time and require large amounts of data. Lumped models do not have this problem, but may be less accurate. The BQART model, for example, is a semi-empirical model which estimates the sediment load of a river using several factors and is easy to use. However, it was intended to be used for whole basins at a decadal timescale. The aim of this study was to test whether the BQART model is accurate at a monthly timescale and whether it can be used for smaller catchment areas. A second aim was to evaluate whether adding a bank erosion term would improve the model's predictions. In order to test this, the model was implemented for the Mekong, which is a river that has seen a large decrease in sediment concentration due to the construction of many dams in China, Laos and Vietnam. The river was divided into subcatchments, to which the BQART equation was applied at along with a new bank erosion term. This bank erosion term assumed a constant rate of bank retreat along the length of the major river branches. The calculated sediment loads for these catchments were added together to obtain a timeseries of the monthly sediment load in the Mekong. The model was then calibrated and validated using existing data. The model showed promising results and managed to predict the decreasing pattern in sediment load rather well. The average sediment load values were within the ranges found by previous studies. However, sediment load peaks were underestimated. The model also still has several limitations and problems that still need to be resolved, such as an overestimation of sediment contribution from the delta. The bank erosion term proved less useful due to the many assumptions that were made in order to implement it with the current lack of data. If these issues can be resolved, the sediment load can be more accurately predicted and the model can be used to get more insight into smaller scale sediment dynamics.

Contents

Abstract 2

1. Introduction 4

2. Study area 6

2.1 The Mekong 6

2.2 Climate 10

3. Methods 13

3.1 The BQART model 13

3.2 Bank erosion 14

3.3 Model data 16

3.4 Calibration and validation 16

4. Results 19

4.1 Uncalibrated results 19

4.2 Calibration results 21

4.3 Model validation 25

5. Discussion 27

5.1 Interpretation of the model output 27

5.2 Model limitations and inaccuracies 28

5.3 The bank erosion factor 30

6. Conclusion 31

7. References 33

1. Introduction

The sediment concentration in rivers worldwide has significantly decreased in recent decades (Dunn et al., 2019). This decrease is caused by better soil conservation practices as well as an increase in the amount of dams and reservoirs (Dunn & Minderhoud, 2022). Reservoirs have an increased sediment trapping efficiency, which results in a loss of sediment downstream (Vörösmarty et al., 2003). This enhanced trapping efficiency is caused by the lower flow velocity within a reservoir.

Sediment deposition in the delta area results in an increased coastal elevation. Due to increased absolute sea level rise and the lack of sediment input from rivers, this increase is currently being outpaced by relative sea level rise in many of the world's delta regions. This effect is enhanced by loading and the extraction of oil and drinking water, which results in subsidence (Minderhoud et al., 2017). The higher relative sea level leads to increased flooding and salt intrusion, which may cause substantial damage to coastal areas, resulting in tremendous costs and possibly loss of life. The salt intrusion can also lead to even higher water requirements, which may result in even more water extraction from the ground and this can cause even more subsidence in a positive feedback loop. A lack of sediment can also cause a reduction in the fertility of the delta's which may have a large negative impact on food security (Romero-Díaz et al., 2012).

The addition of adequate amounts of sediment by flooding delta areas in a controlled manner so sediment can be deposited there again may help prevent such a scenario (Dunn & Minderhoud, 2022), especially if this is combined with measures to prevent further decrease subsidence due to groundwater extraction. Sediment deposition itself also causes more loading of the surface and therefore more sediment is required than the desired difference in elevation.

Due to the decreasing sediment concentration, there is currently not enough sediment to sustain such measurements, which means a method must be found to increase the sediment availability. The sediment delivery may be increased by decreasing the amount of reservoirs or decreasing the amount of channel mining. Sediment transport patterns can also be altered by changing the amounts of water flowing to different regions of the delta as part of a controlled flooding scheme.

In order to find and implement appropriate measures to increase sediment delivery to the delta, the sediment concentration must first be accurately modelled. By using distributed models, the sediment concentration over an entire river network can be modelled at precise locations. However, this requires much computing power and time, which may also have more financial costs. Lumped models may contain less information, but they also require less computing power and can be run faster, which may make them more useful when combined with other models and/or to complete more model runs for different scenarios.

One such model is the BQART model created by Syvitski and Milliman (Syvitski & Milliman, 2007). BQART is a lumped model that calculates the suspended sediment load (SSL) of a river based on empirical relationships between the sediment load and the discharge, basin area, elevation differences and temperature. The model also includes a factor to account for basin

geology, erosion by glaciers, sediment trapping by reservoirs and human influences on erosion. These relationships were established by comparing data on these factors with SSL data across the world.

The BQART model was intended to be used on a timescale of decades for entire basins. However, in order to obtain knowledge about intra-annual sediment dynamics, a monthly timescale would be required. This knowledge could be valuable to sedimentation strategies such as controlled flooding. With knowledge of when the sediment concentration is largest, one could plan a more precisely controlled operation, potentially decreasing costs or increasing benefits of such a strategy. However, no one has attempted to use the BQART equation at a smaller timescale yet.

The model may also be useful at smaller spatial scales in order to investigate the sediment contributions of subbasins to the larger catchment. This could enable one to easily track where the greatest reductions in sediment load occur. This could be necessary knowledge to increase the sediment load of a river. Again, no one has investigated whether the BQART model also works at such a spatial scale.

The BQART equation does not include every component that enhances sediment erosion. Bank erosion, for example, can be a large component of the sediment load of a river, especially when the base sediment concentration of a river is low. However, the model does not incorporate bank carving by the river as a factor in its estimation of erosion enhancing factors. The model could therefore be improved by adding a component that predicts the amount of sediment produced by bank erosion.

The aims of this thesis are to assess whether the BQART model could work accurately on a monthly timescale as well as a smaller timescale and to evaluate whether adding a component representing bank erosion would enhance the model's performance.

2. Study area

2.1 The Mekong

The Mekong river has a total length of 4800 km, and is thus the 12th longest river in the world. It has the 8th largest annual runoff, which is 470 km^3 (Sok et al., 2021). The total basin area is 795000 km^2. The river flows through China, Myanmar, Laos, Thailand, Cambodia and Vietnam and has great economic importance, especially for fishery and agriculture (Figure 2.1).

Figure 2.1. The location of the Mekong basin (Open Street Maps). The delineation shown here is slightly inaccurate, as it results from an ldd which includes only part of the delta area. The area is thus actually slightly larger.

The Mekong is known in China as the Lancang (Jiang) river. It originates at Chamdo in Tibet, at the confluence of the rivers Angqu and Zha Qu, before flowing through the Yunnan province (Figure 2.2). It forms the border between Myanmar and Laos, then flows through parts of the Laotian mountains. At Pak Ou, the river Nam Ou flows into the Mekong. These upper parts of the river are heavily incised.

Near Vientiane, the river starts to develop a floodplain and has a meandering pattern. Throughout this section, which is on the border between Laos and Thailand, the Mekong is joined by several major tributaries: The Nam Ngum, Nam Ngiap and Namkading rivers, which all originate in the Annamite mountains to the north and east of the Mekong.

The Mun river is the largest tributary, it originates in Thailand, its confluence with the Mekong is at Khong Chiam. The Mun itself also has several tributary rivers, including the Chi and Srebok rivers.

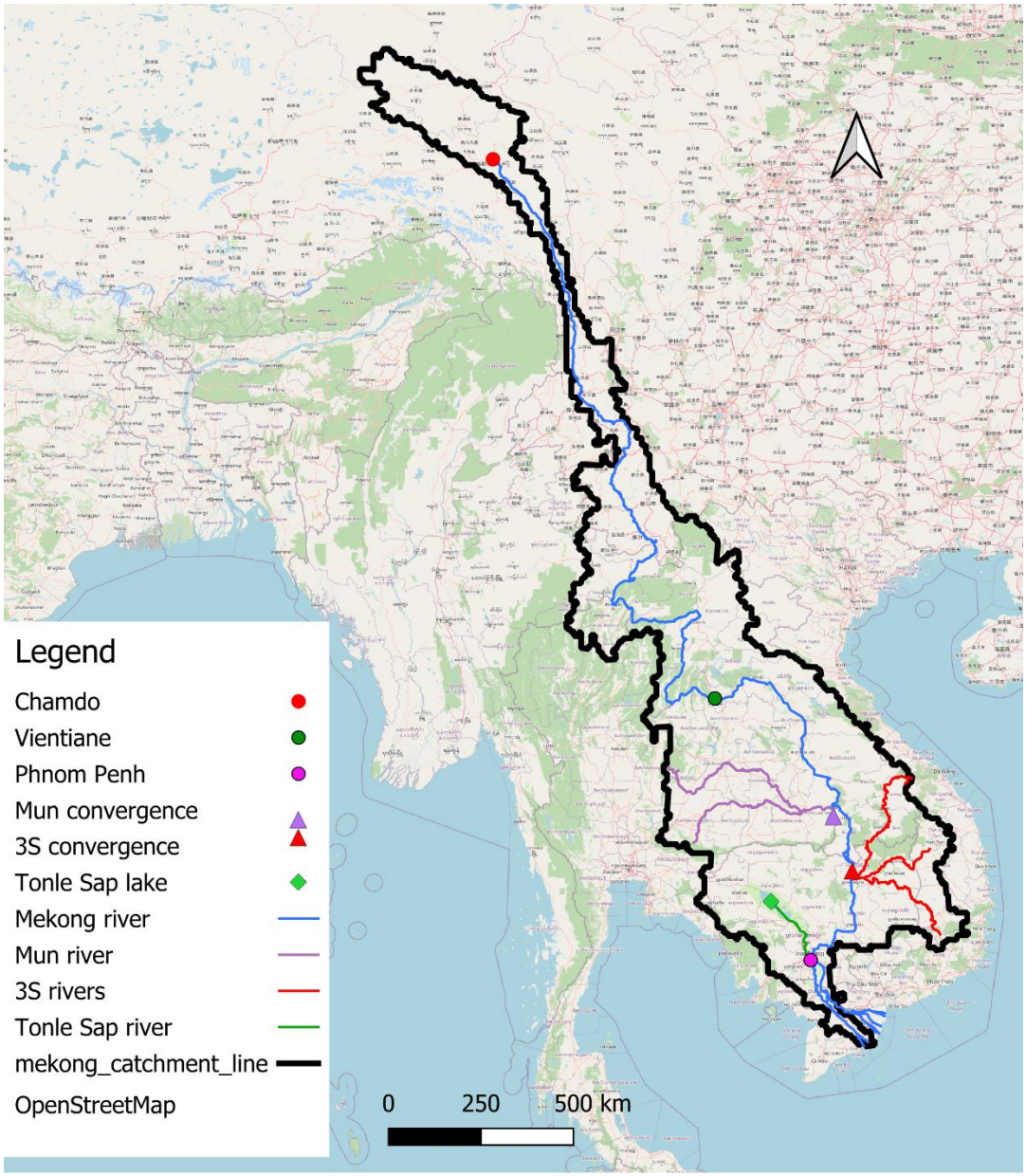

Figure 2.2. Map of the Mekong and the tributary rivers considered (Open Street Map). The Chi river has been combined with the Mun river as they are part of the same system. For similar reasons, the Bassac river is grouped with the Mekong river.

The Sekong, Sesan and Srepok rivers (also known as the Tonlé Sekong, Tonlé (Se) San and Tonlé Srepok/Dak Krong rivers respectively) are major tributaries that merge before the confluence with the Mekong at Stung Treng and are thus usually taken as one tributary system. All three rivers originate in Vietnam and enter the Mekong in Cambodia, however, the Sekong also flows through Laos. The combined river system will be referred to as the 3S-system in this thesis.

Tonlé Sap river is more complicated as its flow reverses depending on the difference in water levels between the Mekong and Tonlé Sap lake (Sok et al., 2021). When the water in the Mekong is higher the river acts as a distributary and the lake acts a sink, but when it is lower the river becomes a tributary instead and sediment deposited in the lake can be eroded again and it becomes a source of sediment. Generally, the reversed flow occurs from May to October (Carling, 2009). The inflow of water and sediment from the Mekong results in an increase in productivity for Tonlé Sap Lake and is important for the fishing industry there (Kummu & Koponen, 2008).

Slightly downstream, at Phnom Penh, the Bassac river distributary branches off from the main Mekong river. In Vietnam, this river is instead known as the Hau river. At Vĩnh Long, the river again splits between the main Mekong in the North and the Cổ Chiên distributary in the South.

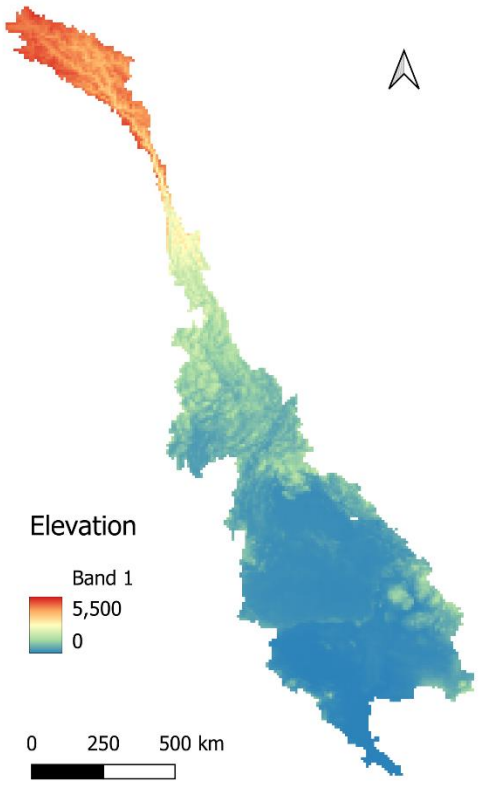

Figure 2.3. Digital Elevation Model of the Mekong catchment. Data from the PCR-GLOBWB model (Sutanudjaja et al., 2018).

The Mekong is affected by several elevated regions (Figure 2.3). The highest of these is the Tibetan Plateau, where the Mekong originates. The upper parts of the Mekong also flow through the rugged Yunnan Province in China. The eastern parts of the Mekong are bounded by the Annamite mountains, in which many tributaries originate, including the 3S-system. These regions are the main source of sediment in the Mekong. They also contain most of the reservoirs.

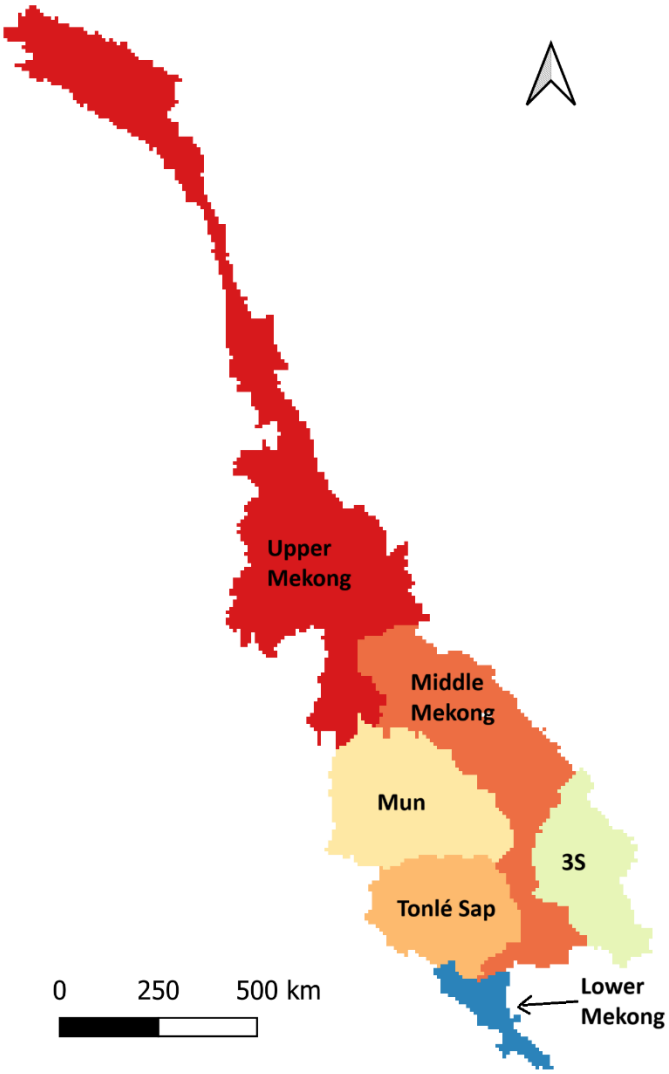

Figure 2.4. Map of the subcatchments of the Mekong considered in this study.

For the purposes of this study, the main Mekong river will be divided into three parts, the Upper Mekong, from its origin to Vientiane, the Middle Mekong, from Vientiane to Phnom Penh and the Lower Mekong, which constitutes the delta. The study will also incorporate the Mun river, Tonlé Sap river and lake and the 3S rivers as subcatchments of the Mekong(Figure 2.4). Other tributaries will be merged with the section of the main river where they join. This gives us six subcatchments in total.

2.2 Climate

Most of the Mekong catchment is located in the tropics and experiences year-round temperatures of above 20 degrees. The southern areas, including the delta, Tonlé Sap and 3S subcatchments, experience higher temperatures than the ones located more towards the north (Figure 2.5). The upper section differs from the other subcatchments. Here the average temperatures per year are between 13 and 16 degrees, which is much lower. This is caused both by its more northern location and its higher elevation.

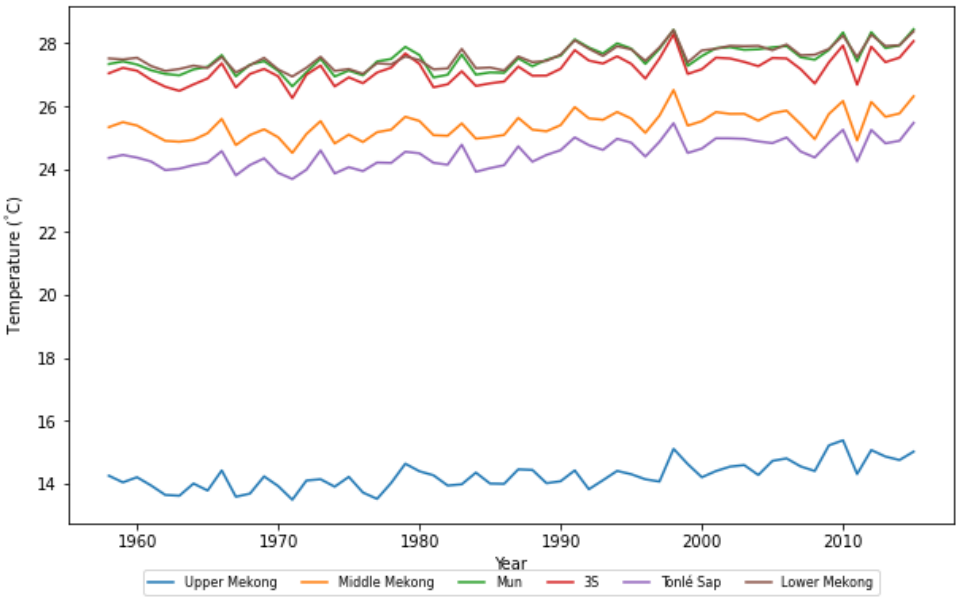

Figure 2.5. Average annual temperature from 1958-2015 in every subcatchment. Data from the PCR-GLOBWB model (Sutanudjaja et al., 2018).

The difference between the maximum and minimum temperature in a year is also higher in the Upper Mekong section (Figure 2.6). More mountainous subcatchments generally seem to experience larger temperature fluctuations than those with small elevation differences.

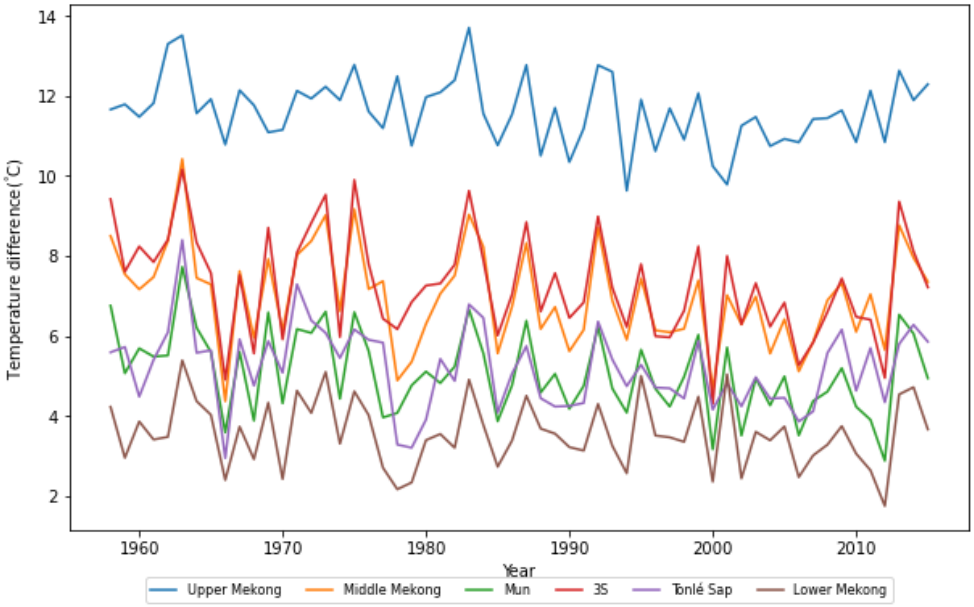

Figure 2.7. Difference between the maximum and minimum temperature per year from 1958-2015 for every subcatchment. Data from the PCR-GLOBWB model (Sutanudjaja et al., 2018).

Most of the Mekong catchment experiences a tropical monsoon climate, which means that the precipitation pattern shows a strong seasonality due to shifting general wind directions. Most of the catchment receives more precipitation during the summer months when the wind direction is from the southwest. This timing is also consistent with higher discharges in the Mekong and the flow reversal in the Tonlé Sap river. The region is also affected by tropical cyclones (Darby et al., 2016).

The 3S subcatchment receives less precipitation due to its location on the lee side of the Annamite mountains (Figure 2.6). The Middle Mekong subcatchment is located on the windward side of these same mountains and receives more precipitation than the Mun subcatchment. The Tonlé Sap and Lower Mekong subcatchments lie close to the Indian Ocean, which also results in more precipitation than the Mun subcatchment, which lies much further away. The Upper Mekong receives less precipitation. Its predominant wind direction is from the northeast and its location far from the China Sea results in drier air. Its location outside the tropics also results in less convective precipitation although the region does have orographic precipitation due to its mountainous nature.

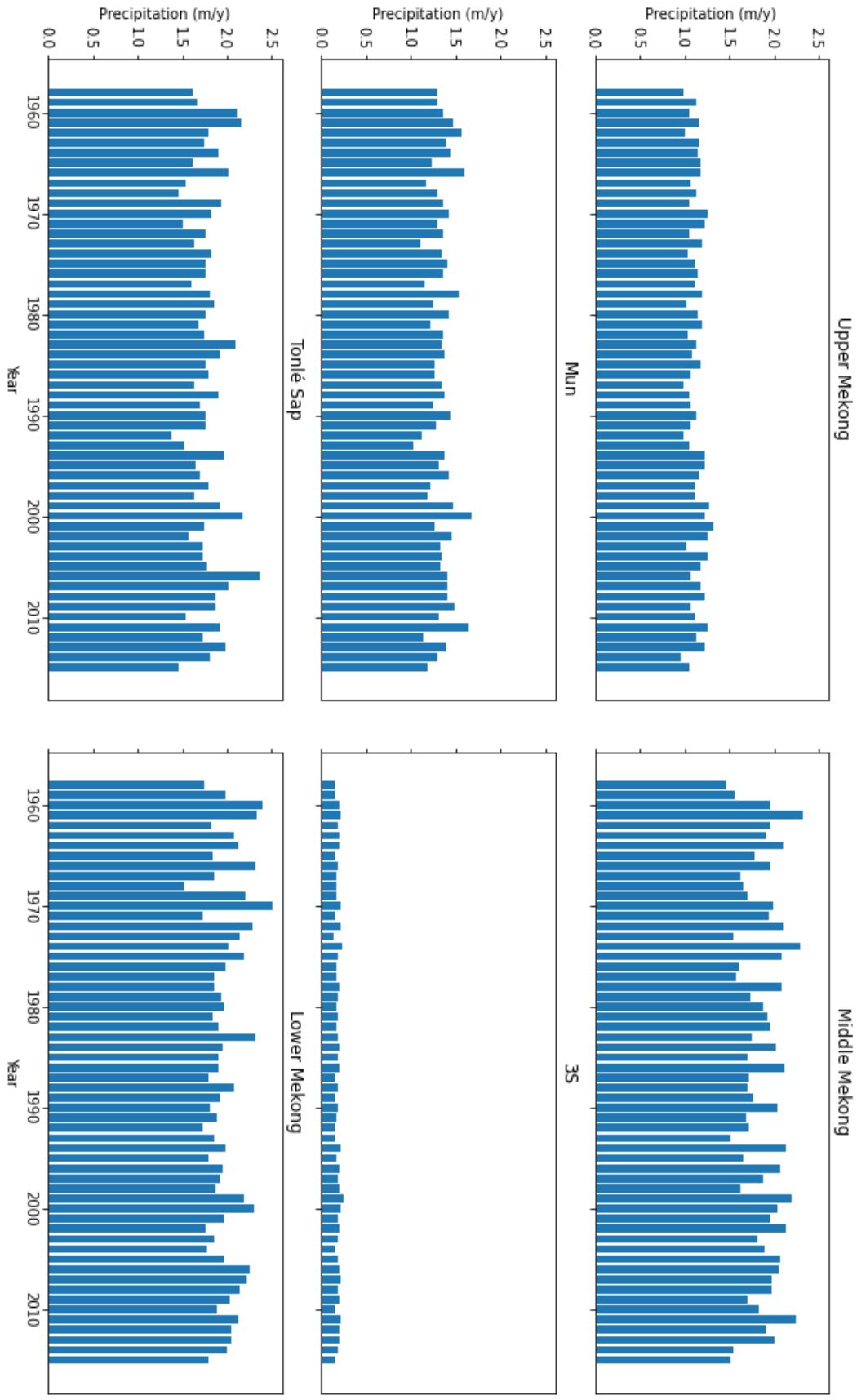

Figure 2.7. The average annual precipitation per m^2 in every subcatchment from 1958-2015. Data from the PCR-GLOBWB model (Sutanudjaja et al., 2018).

3. Methods

3.1 The BQART model

In this study, the BQART equation will be used to calculate sediment transport (Syvitski & Milliman, 2007). It is important to note that the model calculates the total sediment load based on empirical relationships and is thus very simplified.

Time is not included as a factor, which means that several delays between processes are not included. Firstly, the delay between increased discharge or temperature and sediment erosion is not included. It takes time for the increased erosive power to lead to increased erosion. Secondly, it is also assumed that the eroded sediment is immediately added to the main Mekong river branches, while in reality, the eroded sediment is first transported by overland flow and minor river branches. This delay can be in the order of hours to days depending on where the sediment originated.

The BQART equation is written as

$$Q_s = \omega B Q^{0.31} A^{0.5} RT \quad \text{for T} \geq 2\ ^\circ\text{C}, \tag{3.1a}$$

and

$$Q_s = 2\omega B Q^{0.31} A^{0.5} R \quad \text{for T} < 2\ ^\circ\text{C}, \tag{3.1b}$$

where Q_s is the sediment load, Q the discharge in km^3/yr, A the drainage area in km2, R the maximum relief in km and T the average temperature in the basin in ˚C. ω is a factor with a value of 0.02 if Q_s is in kg/s or 0.0006 if Q_s is in MT/yr. The factor B accounts for other geological or human factors of importance. It is calculated as

$$B = IL(1 - T_E)E_h, \tag{3.2}$$

where I (-) represents erosion by glaciers, L (-) the lithology, T_E (-) the trapping efficiency and E_h (-) soil erosion due to human influence. The factor I is calculated as follows:

$$I = 1 + 0.09A_g, \tag{3.3}$$

where A_g is the glacier covered area as percentage of the total basin area. Both the lithology and human factors were set to 1.0 (Dunn & Minderhoud, 2022).

The trapping efficiency is calculated using two equations. If the reservoir volume is below 0.5 km^3, Brown's equation is used (Kettner & Syvitski, 2008):

$$T_E = 100\left(1 - \frac{1}{1+0.0021D\frac{C}{W}}\right), \tag{3.4}$$

where C is the reservoir capacity and W the basin area upstream of the reservoir. D is a factor determined by the geometry of the reservoir. Here it is taken as 0.1. If the reservoir volume is larger than 0.5 km^3, Vörösmarty's modified version of Brune's equation is used to calculate the trapping efficiency (Vörösmarty et al., 2003):

$$T_E = 1 - \frac{0.05}{\left(\frac{C}{Q}\right)^{0.5}}. \quad (3.5)$$

Both the PCRGLOB-WB model and the BQART model do not take the flow reversal in Tonlé Sap River into account. Therefore the assumption was made that the flow reversal always occurs during the months that typically have a high discharge (May to October). Since accurate discharge data for the reversed flow was not available, it was also assumed that the discharge that flows from the Mekong to the lake is the same as it would be for flow from the lake to the Mekong. The relief was also also assumed to be the same. The BQART and bank erosion terms were thus calculated as normal, but taken as negative since the flow direction is reversed. Flow from November to April was assumed to be normal.

3.2 Bank erosion

The BQART model will be altered to include a factor to represent bank erosion. Bank failure may add sediment to the river. This additional sediment is equal to the volume of bank erosion and/or collapse (Thorne & Osman, 1988).

$$\frac{\partial Z}{\partial t} = \frac{-1}{1-\lambda}\frac{\partial q_s}{\partial x}. \quad (3.6)$$

Here Z is the river bank elevation (m), x is the length of the river section and λ is the bed porosity (-). This equation assumes there is no change in width and is therefore two dimensional. By adding floodplain width as a factor, a three dimensional model can be created. If we assume width changes instead of bank height, the rate of change in width over time is calculated as follows (equation 3.7):

$$\frac{\partial q_s}{\partial x} = Z(\lambda - 1)\frac{\partial y}{\partial t}, \quad (3.7)$$

where $\frac{\partial y}{\partial t}$ is the erosion rate (m/y), Z is the bankful depth and ∂x the river bank section taken (Figure 3.1). It is assumed that the bank erosion occurs only.

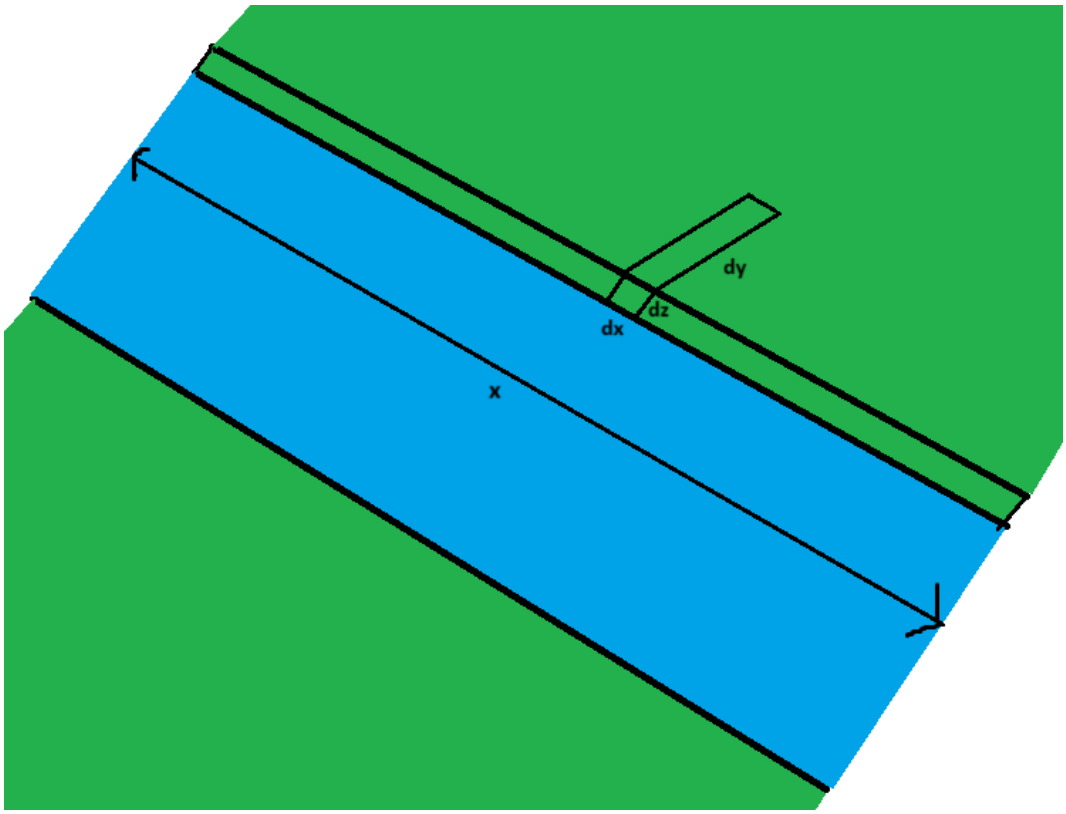

Figure 3.1. Explanation of the spatial factors used in equation (3.7). Here, dx is a small section of the river length, dy the eroded width and dZ the bankful depth per time step.

Naturally, sediment may also be deposited along a river in river bends or during floods. The river banks therefore act as temporary storage. Therefore, what must really be taken into account is the net amount of sediment exchange. The amount of sediment entering the river is smaller than the extent of the eroded bank as deposited sediment contains pores. The bed porosity λ is calculated as

$$\lambda = 0.245 + \frac{0.0864}{{D_{50}}^{0.21}}. \tag{3.8}$$

The D_{50} for bank material samples seems to vary between 0.01 and 0.08 mm with an average of about 0.022 mm (Luu et al., 2004). It should be noted that finer sediment may be found in the delta region. Within delta floodplains, the medium sediment size varies between 10 to 15 µm (Hung et al., 2014; Manh et al., 2014). In this study, the average of 0.022 mm ($2.2 * 10^{-5}$ m) will be used.

The erosion rate was calculated using van de Wiel's equation (van de Wiel, 2003).

$$\frac{\partial Z}{\partial t} = 0.053 * A^{0.44}, \tag{3.9}$$

where A is the basin area. Adding the bank erosion term to the BQART term results in the total sediment load per subcatchment.

$$Q_{s,total} = Q_{s,BQART} + Q_{s.erosion} \tag{3.10}$$

This method was chosen due to data availability and its easy linear use. A complete bank erosion model would rely too much on equilibria between forces at any time and place along the river and would both require too much computational power and data. Such a bank erosion model would also be a discrete, physical model and would not fit well with the BQART model, which is semi-empirical. The precise, quantitative relationship between bank erosion and the total sediment load of a river is unknown, therefore it is impossible to implement bank erosion in the BQART equation itself. A rough estimate is the next best method and was therefore applied in this study.

3.3 Model data

The discharge, temperature, snow cover and topographical data are reused data from the model runs from Sutanudjaja et al. in 2018. They developed a new version of the PCR-GLOBWB 2 model, which is a global hydrological model (Sutanudjaja et al., 2018). Their model runs contained data on the circumstances in various sections of the Mekong river and modelled discharge data based on this. The resolution of this data is 5 arcmin.

All data on reservoirs are the same data used in the study by Dunn and Minderhoud (Dunn & Minderhoud, 2022). Every dam was sorted into the corresponding subcatchment and the total reservoir area in each subcatchment was calculated for every year. It was assumed that all dams were built at start of the listed year.

3.4 Calibration and validation

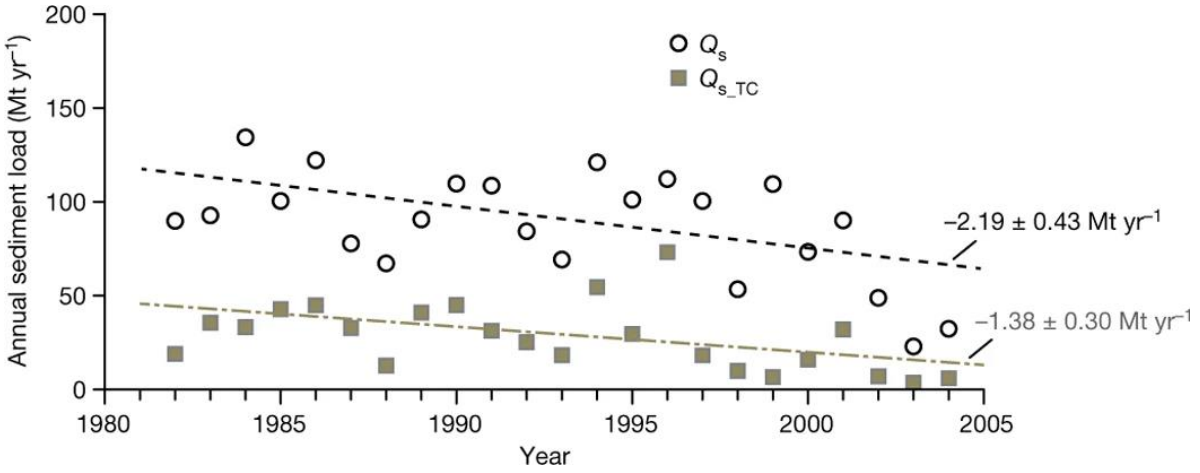

Figure 3.4. The sediment load data represented by the white circles was used as calibration data (Darby et al., 2016).

Timeseries data on the Mekong's sediment load for a larger interval turned out to be unexpectedly sparse, considering the amount of studies focusing on sediment load over smaller intervals. Because most useable data included Kratie as measuring location, the decision was made to calibrate the model using data for Kratie. Kratie lies slightly upstream

from Phnom Penh, between the Mekong's confluences with the 3S rivers and the Tonlé Sap river. Since the floodplain in Cambodia has no strong elevation gradient (Figure 2.3), the Mekong has much less erosive power here and the difference in sediment load between Kratie and the confluence with the Tonlé Sap at Phnom Penh is likely to be insignificant. Therefore it was assumed that the sediment at Kratie equaled the sediment at Phnom Penh without the sediment load of the Tonlé Sap:

$$Q_{s,Kratie} = Q_{s,PP} - Q_{s,TS}$$

The goal function used for calibration is the Nash-Sutcliffe efficiency (NSE) (Nash & Sutcliffe, 1970;Duc & Sawada, 2023):

$$NSE = 1 - \frac{\sum(o_i - s_i)^2}{\sum(o_i - \mu_o)^2}, \tag{3.11}$$

where o_i is the measured value and s_i the modelled one. μ_0 is the average value of the measurements.

An NSE equal to 1 represents a model that perfectly predicts the measured data, which is practically almost impossible to achieve. An NSE between 0 and 1 means that the model is a better predictor of the measured data than the average value of that data, while an NSE lower than 0 indicates that the average value is the better predictor. In that last case it is possible that the model is either wrong or not working properly.

When using the NSE for calibration, the model is run for different calibration factors.

$$Q_{s,total} = (Q_{s,BQART} + Q_{s.erosion}) * c_f. \tag{3.12}$$

The correct calibration factor is the one that results in the highest NSE, as this leads to the most accurate model. This method is not ideal as this may in some cases overfit a model. An attempt to calibrate one of the parameters in the BQART equation, namely E_h (equation 3.2), was made, but led to errors in the resulting data. Therefore, the calibration factor method was chosen as it was easier to implement. The calibration factor multiplies both the BQART equation term and the bank erosion term with the same factor. Since Q_s in the BQART equation linearly increases with the E_h and L factors, the result of this multiplication is the same as calibrating E_h. The bank erosion term is treated as if multiplied by a parameter with the same value. Since the bank erosion term is much smaller, it is assumed that calibrating it individually does not significantly add to the model accuracy.

The model must also be validated. This will be done with data from various studies including the study by Van Binh et al., which was one of the only studies that included a timeseries of measured data (Van Binh et al., 2020). The model will also be compared to model outcomes from a study that used the BQART model at its intended scale.

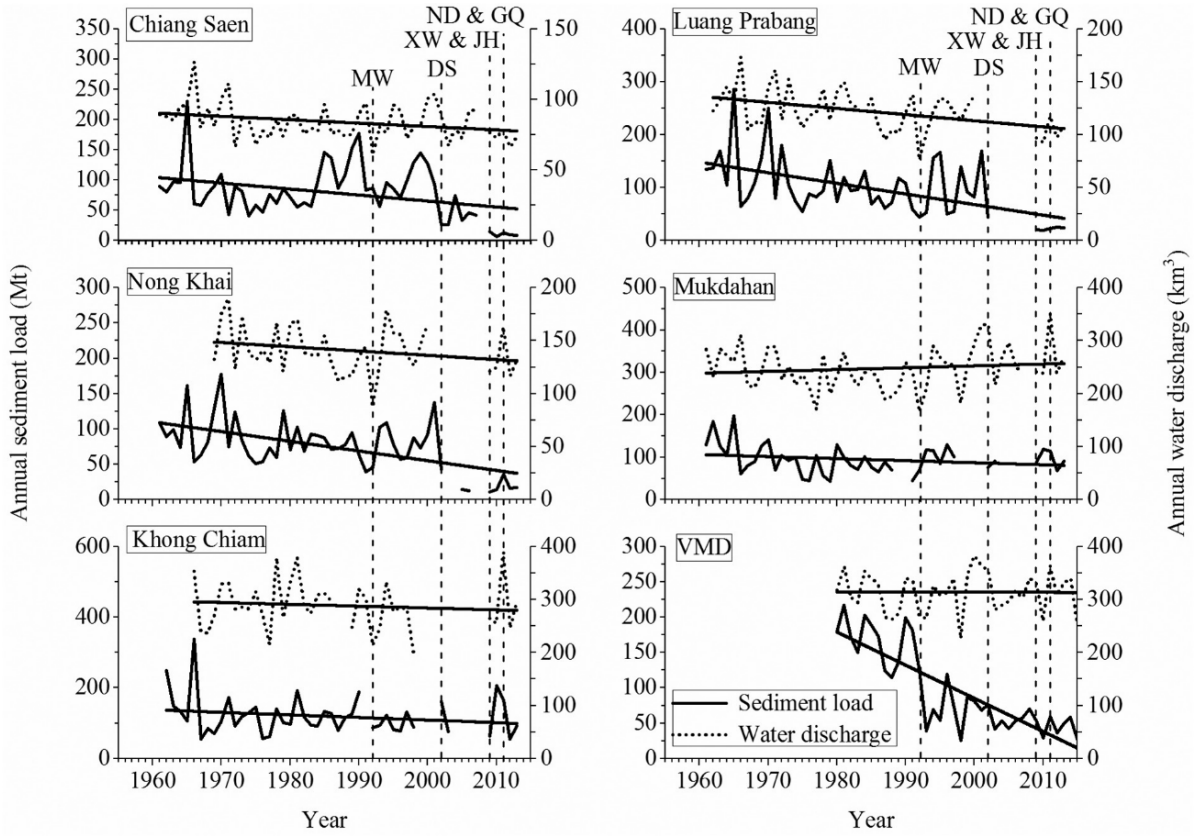

Figure 4.4. The sediment load data in the lower right graph was used as validation data (Van Binh et al., 2020).

4. Results

4.1 Uncalibrated results

The modelled sediment load for the Mekong shows a declining trend (Figure 4.1). The visible peaks represent the largest sediment load per year. Likewise, the troughs correspond to the lowest sediment load. Within the general decreasing trend, the peaks tend to seemingly randomly vary.

The sediment load added to the Mekong within its middle section shows a large drop in 1971, which was also visible in the total sediment load of the Mekong (Figure 4.1). There are more, smaller decreases in the 2010s. These smaller declines are less abrupt than the one in 1971.

The sediment load of the Mun river experiences a seemingly even more abrupt decrease in sediment load due to its already lower initial load (Figure 4.1). The sediment load due to bank erosion is relatively high in the Mun.

Another large decrease in the sediment load of the Mekong occurred between 1997 and 1999 in the 3S river subcatchment (Figure 4.1). Bank erosion is relatively low compared to the total load before 1998, but large compared to the load after.

The plot for the Tonlé Sap River shows two peaks (Figure 4.1). One positive peak during the winter months and one negative one during the summer months. The negative sediment load is larger, which means that there is net sediment transport away from the Mekong towards Tonlé Sap Lake. The bank erosion also occurs in both direction, but since the rate is constant its net effect is zero.

The Mekong delta shows no decreasing pattern (Figure 4.1). The contribution by bank erosion is again almost negligible. As the sediment additions in the delta do not show the decreasing pattern, the trend visible in the sediment load at Phnom Penh is the same as at the end of the Mekong. Of note is that the bank erosion term has a larger relative contribution here than at the end of the river, likely because there is very little bank erosion in the Mekong delta.

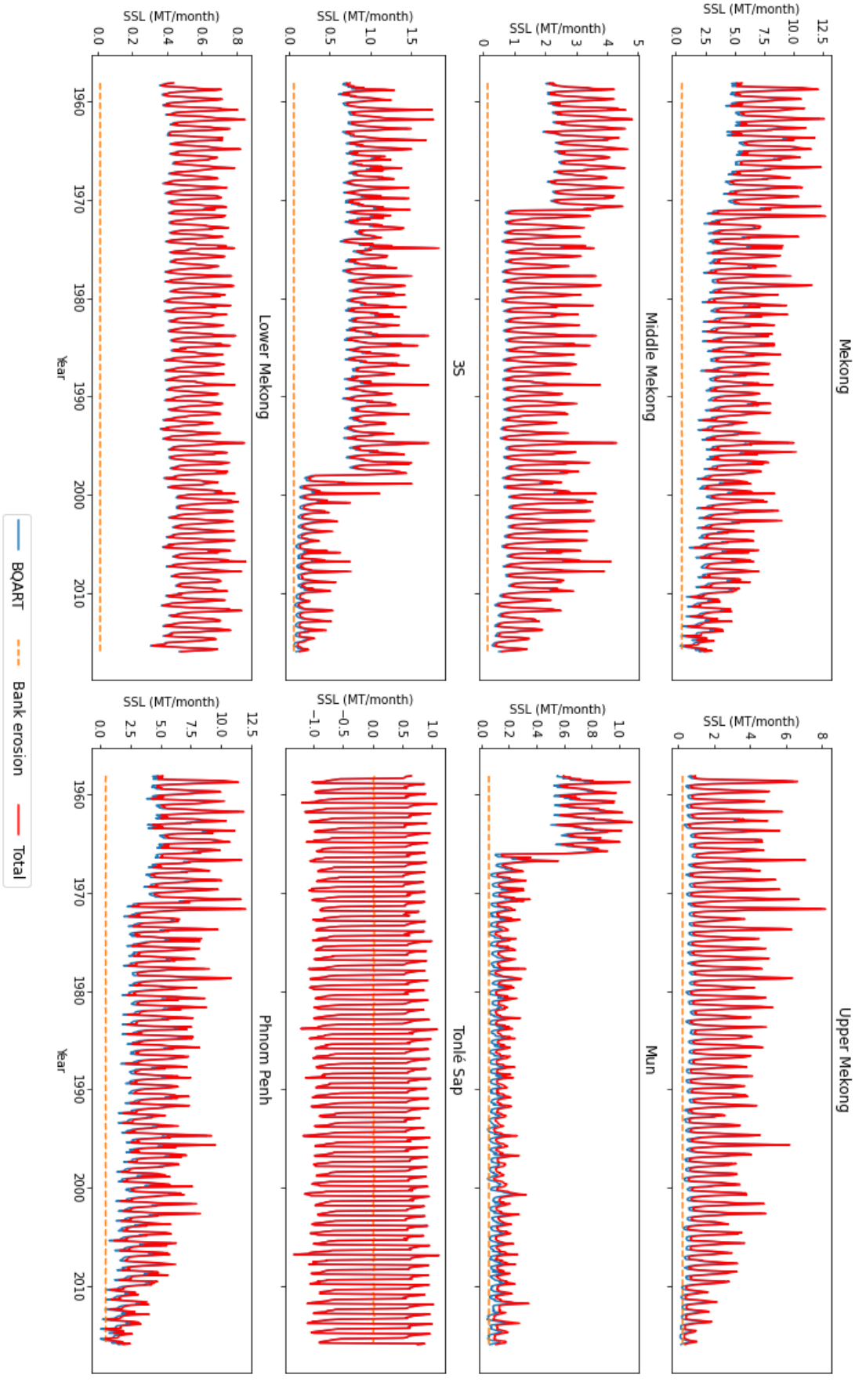

Figure 4.1. The SSL of the Mekong and its subcatchments per month from 1958-2015 as calculated by the uncalibrated model.

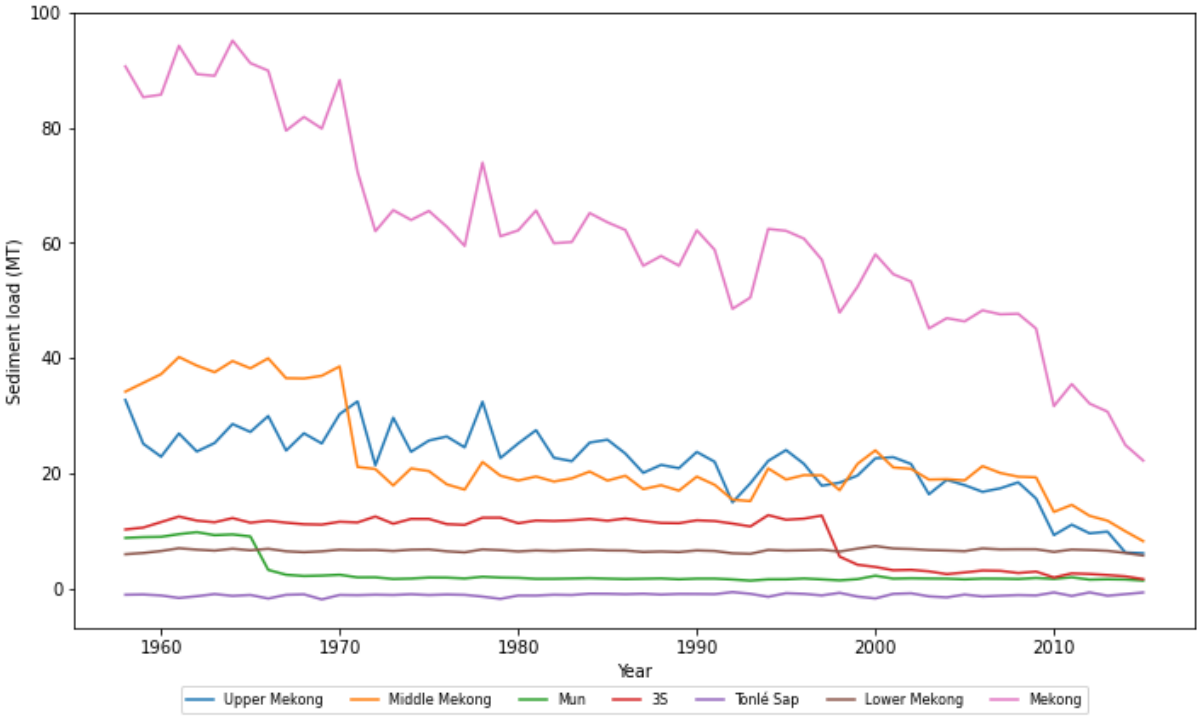

Figure 4.2. Sediment load of the Mekong compared to that of the subcatchments on a yearly scale.

The largest part of the sediment load is contributed by the Upper and Middle sections of the Mekong (Figure 4.2). The Tonlé Sap River contributes the least on a yearly basis, which is due to the flow reversal. The 3S tributaries contribute more than the Mun, but their sediment load has been significantly reduced by reservoir construction in the late 1990s. A similar decrease in sediment load occurred in the mid-1960s for the Mun.

4.2 Calibration results

The initial, uncalibrated model had an NSE of -1.49589 *(Table 4.1)*, which means the model did not result in a good prediction of the data. Calibration improved this to an NSE of 0.428728, using 1.78 as value for the calibration factor *(Table 4.1; equation 3.12)*. This means that the model decently predicts the data, but could be improved.

Table 4.1. Calibration factors and corresponding NSE for the model. The first and second model contain information from the first calibration run, the third and fourth from the second, more specific calibration run. The calibration factors corresponding to the highest NSE are in bold.

Calibration factor	NSE	Calibration factor	NSE
0	-9.57236	1.70	0.407794
0.1	-8.48111	1.71	0.412616
0.2	-7.45289	1.72	0.416809
0.3	-6.48768	1.73	0.420371
0.4	-5.5855	1.74	0.423302
0.5	-4.74634	1.75	0.425604
0.6	-3.97021	1.76	0.427275
0.7	-3.2571	1.77	0.428317
0.8	-2.60701	**1.78**	**0.428728**
0.9	-2.01994	1.79	0.428508
1.0	-1.49589	1.80	0.427659
1.1	-1.03487	1.81	0.426179
1.2	-0.636869	1.82	0.424069
1.3	-0.301892	1.83	0.421329
1.4	-0.0299366	1.84	0.417958
1.5	0.178996	1.85	0.413958
1.6	0.324906	1.86	0.409327
1.7	0.407794	1.87	0.404066
1.8	**0.427659**	1.88	0.398175
1.9	0.384501	1.89	0.391653
2.0	0.278321	1.90	0.384501

When comparing the calibrated result to the calibration data (Figure 4.3), the model shows the a similar pattern between 1989 and 1998, except the peak are smaller. This is even more true for the data between 1980 and 1989 where the peak and trough is much smaller and the second peak is not visible. After 1998, the pattern is very different. Where the calibration data shows two separate peaks in sediment load and then rapidly decreases, the modelled data shows one broader peak with roughly the same maximum sediment load as the second peak in the calibrated data and then decreases slowly.

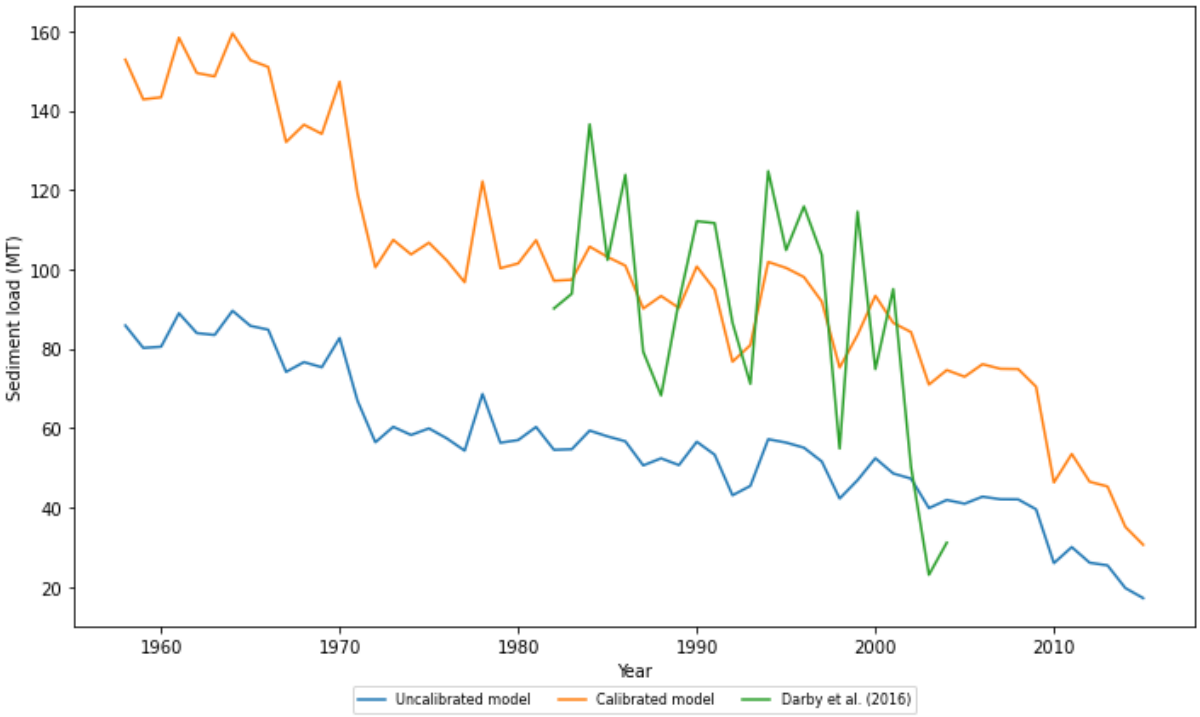

Figure 4.3. The sediment load calculated using the uncalibrated and calibrated models plotted against the sediment load measured by Darby et al. (2016) at Kratie (Darby et al., 2016).

The calibrated version of the model shows that the sediment load used to be above 20 MT per month during the wet season (Figure 4.4). During the dry season the SSL used to be have a minimum of 8 MT per month. This has since become the new maximum value. The new minimum value has become below 1 MT per month, which is a substantial decrease.

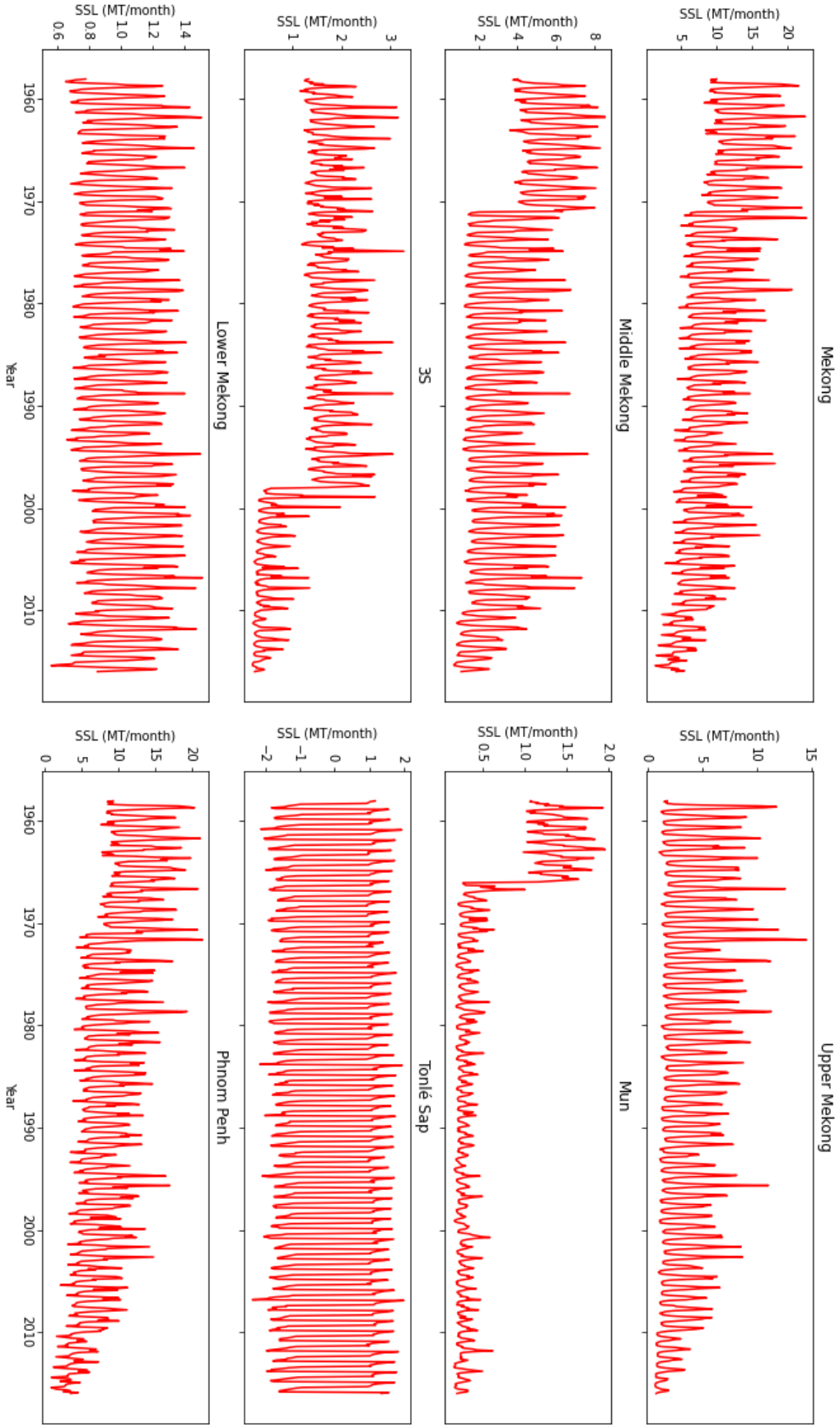

Figure 4.4. Calibrated model for the sediment load in the Mekong and its subcatchments.

4.3 Model validation

In order to validate the model, it must be compared to other, independent data. When compared to data from the study by Van Binh et al., the model again shows a smaller version of most of the sediment peaks and troughs (Figure 4.5). However, the sediment load is much smaller before the early 1990s and somewhat larger after and the model does not show the large decrease shown in the data. This data is thus not predicted well by the model, but it should be noted that the data by Van Binh is also very different from that measured by Darby et al., which means it could be unreliable.

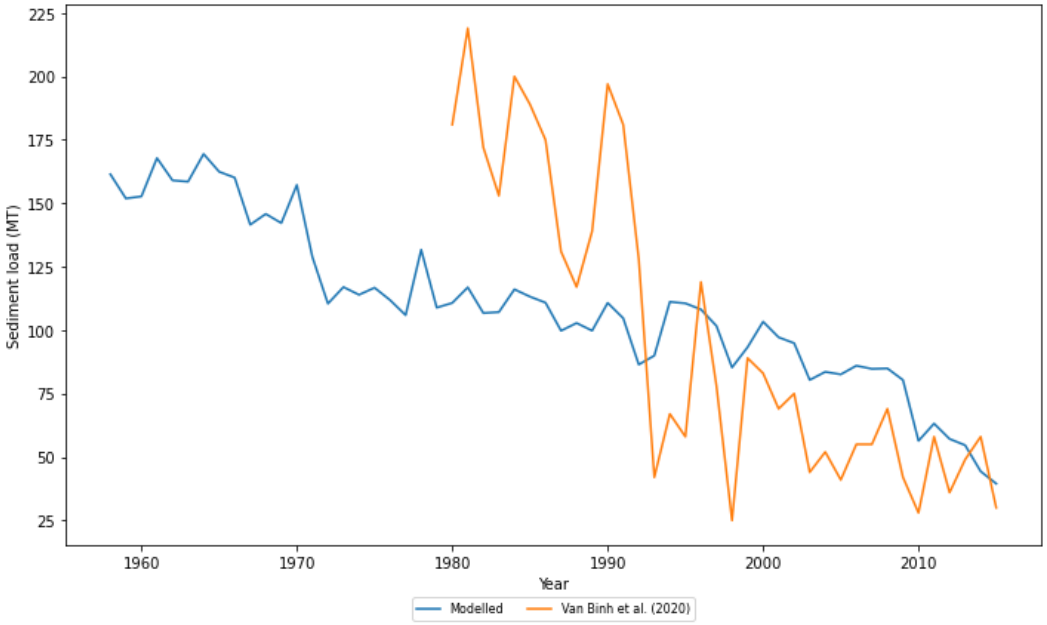

Figure 4.5. Comparison between the model from this study with measured data from the study by Van Binh et al. (2020) (Van Binh et al., 2020).

When compared to non-timeseries data from other studies (Figure 4.13), the model does show similar results. At the start of the modelled timeseries, the sediment load values are similar to the pre-dam values estimated by Liu et al. in 2013 (Liu et al., 2013). The modelled values for 2008 - 2010 also falls within the 50 – 91 MT range estimated by Lu et al. (Lu et al., 2014). However, most values between 1991 and 2003 are above those found by Sok et al. (Sok et al., 2021).

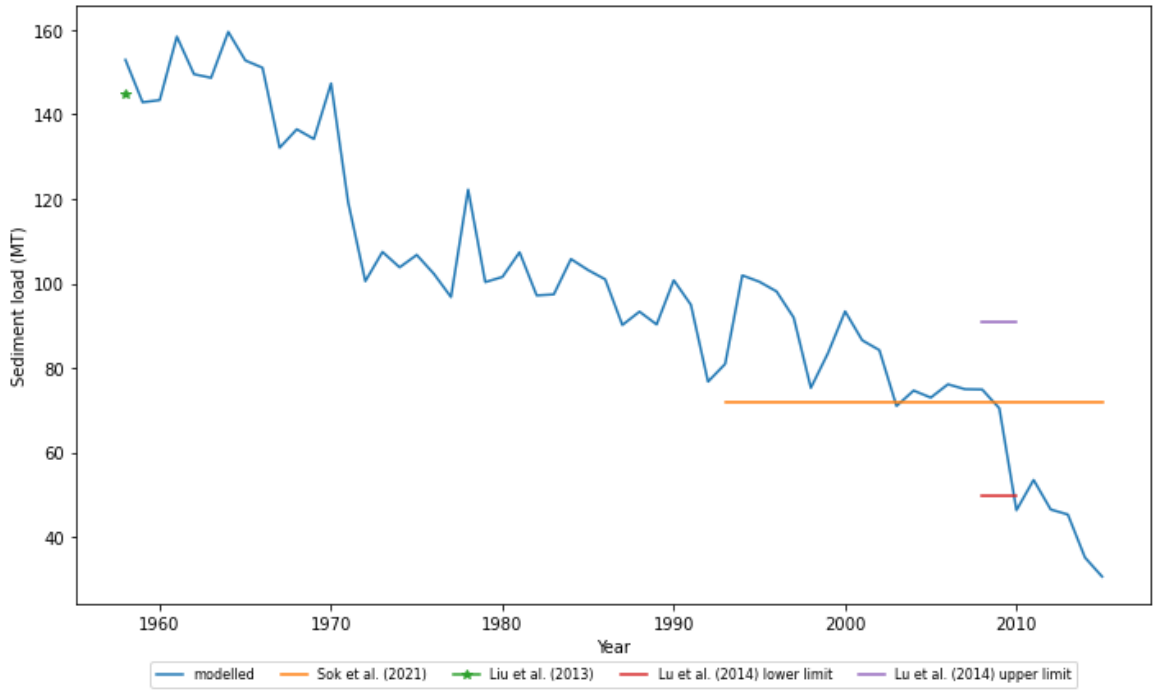

Figure 4.6. Comparison between this model and the values found by other studies (Sok et al., 2021; Liu et al., 2013; Lu et al., 2014)

The model was also compared to the modelling results of a study that used the BQART model at the originally intended decadal scale (Dunn & Minderhoud, 2022) (Figure 4.14). The model outcome is somewhat lower from 1985 – 1995 and slightly higher from 1995 – 2005. The model results lie in between the different scenarios for 2005 – 2015.

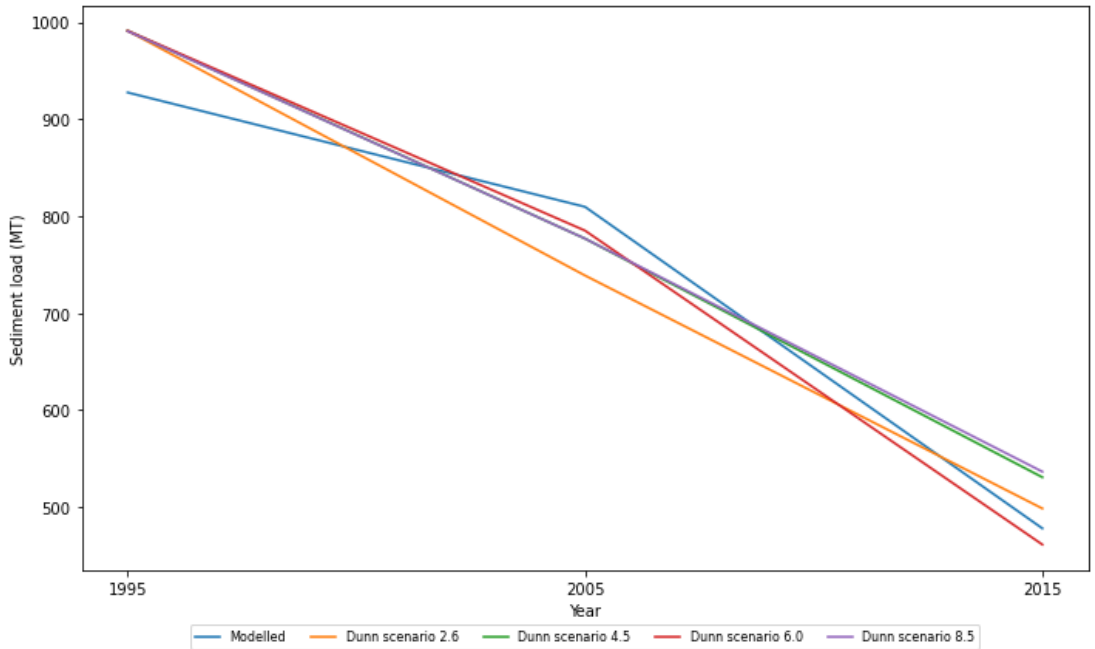

Figure 4.7. Comparison between the model from this study and the model from the study by Dunn and Minderhoud (2022) at a decadal timescale (Dunn & Minderhoud, 2022).

5. Discussion

5.1 Interpretation of the model output

The rapid decreases in sediment load are consistent with the construction of major reservoirs. For example, the decrease in the Middle Mekong corresponds to the completion of the Nam Ngum 1 dam, which with its 4.7 km^3 reservoir volume largely increased sediment trapping (Figure 4.1). In the Mun, the completion of the Ubol Ratang and Lam Pao dams in 1966 and 1968 respectively, led to another massive decrease. Although more dams with large reservoirs were built in the 1970s, these result in only a slight decrease in sediment load, despite leading to an equally large increase in reservoir size.

This implies that the sudden sharp decreases in sediment load are due to the fact that these reservoirs ensure that the total reservoir volume surpasses the 0.5 km^3 threshold. This led to a rapid increase in trapping efficiency. Addition of further reservoirs led to a more general decrease in sediment load for each subcatchment. For example, in the Upper Mekong the decrease is rather gradual, because the total reservoir volume had already surpassed the 0.5 km^3 threshold in 1958. So while new reservoirs were built, they did not have as much of an effect as the ones in other subcatchments.

Within each subcatchment, both the monthly and annual sediment load also varied due to fluctuations in discharge and temperature. In the Upper Mekong, the sediment load also varied due to fluctuations in glacier cover. All these factors taken together resulted in the sediment pattern that was produced by the model for the Mekong catchment as a whole. The different equations for the trapping efficiency are thus the cause for the somewhat unrealistically rough model output.

These thresholds are somewhat unrealistic and a more gradual swap between equations might be needed to smooth them over for the model to show a more realistic outcome in small regions. Perhaps research is required into a better trapping efficiency model around this 0.5 m^3 value for reservoir size.

Despite the model inaccuracies for the Tonlé Sap subcatchment, the results show a net sediment flux towards the lake, which would result in infilling of the lake. This agrees with what was found in previous studies (Kummu & Koponen, 2008; Sok et al., 2021). It is important to note that this is not all the sediment added to the lake as its own tributaries still contribute to the sediment flux during the flow reversal.

While the exact sediment loads are inaccurate during the reversal period, it is clear that the seasonality within Tonlé Sap Lake is very significant and that this also affects the sediment load in the Mekong. If the model output for Tonlé Sap River could be improved, it could be used to better understand the sediment balance within Tonlé Sap Lake and how it is affected by changes upstream in the Mekong catchment, such as dam construction. This could be very beneficial to the people living there, as these developments affect the amount of fish present in the lake and fishery is the main source of income in this region (Campbell et al., 2009). If predictions were to be available at a seasonal scale, systematic measures could be taken to

improve water quantity and quality were necessary, so the lake remains sustainable throughout the year even with the impacts of climate change.

The improved model could also lead to a better understanding of the seasonality of the sediment transport towards the Mekong delta, which could allow for measures that take advantage of momentary sediment load increases to be implemented based on model predictions. For example, better information on sediment availability could be used to accurately decide when to temporarily flood an area in order to increase its elevation (Dunn & Minderhoud, 2022). This could aid in preventing coastal flooding in the delta region.

5.2 Model limitations and inaccuracies

The ldd used to calculate the catchment extent funneled everything into one of the distributaries, which resulted in an inaccurate area for the delta. As a lumped model, the BQART model also does not take distributaries into account. It also ignores tidal dynamics and assumes a constant discharge. Due to this, the calculated sediment contribution by the Mekong delta is unrealistically high. The local discharge should be lower than assumed as the total discharge is spread across the distributaries in reality. The model therefore overestimates the erosive capacity of the water in the delta.

There is a lack of timeseries data for the required locations, which means another solution had to be found. This is why the data for the model run is not measured data but taken from a PCRGLOB-WB run (Sutanudjaja et al., 2018). This means that this data is subject to the limitations of that model. One such limitation is that the timing of the discharge is slightly inaccurate due to the meteorological forcing of that model. This should be taken into account during analysis of the outcome of the BQART model as it impacts the final sediment load.

The BQART model itself is also a semi-empirical model, which means that the model for the most part does not describe actual processes and is very generalised. This means that subtle differences that may influence the parameters, such as rock strain for lithology, are not taken into account (Syvitski & Milliman, 2007).

The human factor of the BQART model is only a rough estimate of human influence. Individual human activities may also influence the sediment load of a river. Other outside influences, such as tropical cyclones and other storms are also not included while their erosive potential can be very large (Darby et al., 2016).

As explained in the methods section, several assumptions were made to calculate the sediment load in the Tonlé Sap river when reversed flow occurs. For example, discharge and relief were These assumptions are inaccurate because the relief is determined from the river stage and discharge is determined by the division at the confluence of the Tonlé Sap with the Mekong and these are all variable and do not rely on conditions within the rest of the Tonlé Sap subcatchment as assumed in this model. Nonetheless, as explained above, the results do agree with previous studies. However, a proper model for flow dynamics in the Tonlé Sap River and Lake should be created, based on the discharge in the Mekong to further improve the

BQART and bank erosion model for this region as well as other regions where such phenomena occur.

Data for the total reservoir discharge per month was also unavailable, which is why the subbasin discharge was used for the trapping efficiency calculation. The discharge for the reservoirs should in reality be much lower as not all discharge in a subbasin passes a reservoir. In addition the upstream area of the reservoirs was also unknown due to the sheer amount of reservoirs, which is why the subcatchment area was used instead. That area is of course too large. Both these decisions will have impacted the trapping efficiency and may be responsible for the sharp decrease in sediment load once the reservoir volume has surpassed the threshold between the two equations.

The choice was made to add a separate calibration factor rather than to calibrate the parameters as is the norm due to the division into subcatchments. Calibrating all subcatchments individually was impossible due to the lack of sediment load data at the required locations and calibrating one parameter for all subcatchments led to errors, leaving the ideal outcome unclear. In future studies, a better calibration method should be found.

A study could be done where the division into subcatchments is different and based on available data rather than natural boundaries. In this case it would be possible to calibrate the same parameter for every subcatchment individually based on local data. This would then lead to a more natural, less forced model result.

The data used for calibration was measured at Kratie. Due to the division into subcatchments, the modelled data used is presumed to be the same as the sediment load at Phnom Penh without the addition of the Tonlé Sap load. However, Kratie is located slightly upstream of Phnom Penh, which means that the actual sediment load at Kratie might be slightly lower in reality. This may have affected the calibration and resulted in a slightly higher calibration factor and slightly higher sediment loads. However, this difference should be very minimal, because as explained in chapter 3.4, the difference in elevation is very low and there are no larger tributaries between Kratie and Phnom Penh.

The model output before calibration was significantly too low. This is either due to the modelled data or due to the BQART equation itself. In these smaller regions, relief differences are likely more significant and these are possibly underestimated in the BQART equation since it assumes a gradual decrease in relief, which in mountainous regions or plateaus is not always the case. Therefore, the sediment load in the Upper Mekong, Middle Mekong and 3S subcatchments may be underestimated. However, the exact relationship between these factors is still mostly unclear and should be further studied (Chakrapani, 2005). The modelled data may have been less variable than the measured data which may have played a large part in the underestimation of the sediment load peaks compared to other studies (Darby et al., 2016; Van Binh et al., 2020).

5.3 The bank erosion factor

The bank erosion shows a trend in its contribution to the total sediment load in a subcatchment. The smaller the BQART sediment load, the larger the contribution by bank erosion will be. The smaller BQART loads are often coupled to smaller catchments. The exception to this is the delta, but since the modelled sediment load may be inaccurate here, that might not mean anything. The bank erosion is also relatively even higher for the Mun due to the Chi. The Mun catchment has a larger river length to catchment area ratio than, for example, the Sesan, Sekong and Srepok rivers when taking only the major river branches into account.

The current model assumes that the bank erosion is constant, however in reality it is very variable. It can, for example, massively increase during flood events. It would also be better to make it a proper empirical factor in the BQART equation rather than a crude addition. This could be accomplished by measuring the discharge and sediment load for a set amount of time before and during a flood event for many small, flat river stretches (to exclude erosion by other factors). The eroded volume of sediment from the bank should also be measured during these periods. In addition, this should be done at catchment scale for multiple and then corrected for the other factors of the BQART equation, which could then result in a relationship between bank erosion, discharge and sediment load. This would then allow the inclusion of bank erosion as part of the B-factor in the model. This could not be done now due to a lack of data.

6. Conclusion

The model shows promising results at this smaller scale. When upscaled it shows a pattern similar to timeseries of measured data from other studies, although the exact peak sediment loads are underestimated. When compared to the output of the BQART model at its intended decadal scale, the predicted sediment load is reasonably similar and falls within the same boundaries.

The sediment load contributed by the delta was overestimated, likely due to the BQART equation relating the entire discharge to erosive power while the discharge in the delta is split into several distributaries and is thus less impactful. An adjustment should be made in order to use the BQART equation for delta subcatchments.

Due to a lack of measured data the choice was made to use modelled data as model input instead, which results in a larger amount of error. The BQART model should be tested at the same scale with measured data in the future to see if this improves its accuracy. A general recommendation would be to do more sediment measurements in the Mekong River and to do so at more locations, so there is more data to use for modelling and calibration. This would prevent many of the issues faced in this study and allow for better research into the dynamics of the Mekong River system.

A future study should also attempt to find a better calibration method, as the current one slightly overfits the model and more specific calibration could lead to more accurate results. With more data available, it should be possible to calibrate the model for each individual subcatchment, which would give the calibration a more solid basis than that which was attempted in this study.

The Tonlé Sap River flow reversal resulted in several problems while modelling that could not be resolved due to a lack of data on the flow dynamics that occur due to this process. While assumptions were made that led to a pattern similar to that found by other studies, an updated model should find a way to implement this dynamic in a better way, so the model predictions become more accurate.

The bank erosion term is not useable in its current state. Too many assumptions were made for it to be a reliable predictor of the amount of sediment contributed by bank erosion and its impact on the total model is relatively small. A better method to estimate bank erosion should be found based on empirical methods. This could make it fit in better with the BQART equation.

Should these issues be resolved, the model will likely be useable at both this spatial and temporal scale as well as for other river systems. This would allow the model to be used to obtain information on smaller scale sediment dynamics and variations in sediment load throughout the year. It could also be used to pinpoint in which subcatchment most sediment is trapped, allowing for more informed decision making when trying to increase the sediment load. This could decrease the cost of policies or increase their benefits. Hopefully, this can be useful in increasing delta sedimentation by pinpointing when and where exactly to apply measures to increase delta sedimentation. Further insight into the Mekong's sediment dynamics will hopefully lead to a better understanding of river systems around the world and

be helpful in creating better models and more accurate predictions. These predictions will be helpful in solving the many problems river and delta regions are currently facing due to climate change.

7. References

Campbell, I. C., Say, S., & Beardall, J. (2009). Tonle Sap Lake, the Heart of the Lower Mekong. In *The Mekong: Biophysical Environment of an International River Basin* (pp. 251–272). Elsevier. https://doi.org/10.1016/B978-0-12-374026-7.00010-3

Carling, P. A. (2009). Geomorphology and sedimentology of the lower Mekong River. In I. C. Campbell (Ed.), *The Mekong: Biophysical Environment of an International River Basin* (pp. 77–110). Academic Press, Elsevier.

Chakrapani, G. J. (2005). Factors controlling variations in river sediment loads. *Current Science*, *88*(4), 569–575. https://about.jstor.org/terms

Darby, S. E., Hackney, C. R., Leyland, J., Kummu, M., Lauri, H., Parsons, D. R., Best, J. L., Nicholas, A. P., & Aalto, R. (2016). Fluvial sediment supply to a mega-delta reduced by shifting tropical-cyclone activity. *Nature*, *539*(7628), 276–279. https://doi.org/10.1038/nature19809

Duc, L., & Sawada, Y. (2023). A signal-processing-based interpretation of the Nash-Sutcliffe efficiency. *Hydrology and Earth System Sciences*, *27*(9), 1827–1839. https://doi.org/10.5194/hess-27-1827-2023

Dunn, F. E., Darby, S. E., Nicholls, R. J., Cohen, S., Zarfl, C., & Fekete, B. M. (2019). Projections of declining fluvial sediment delivery to major deltas worldwide in response to climate change and anthropogenic stress. *Environmental Research Letters*, *14*(8). https://doi.org/10.1088/1748-9326/ab304e

Dunn, F. E., & Minderhoud, P. S. J. (2022). Sedimentation strategies provide effective but limited mitigation of relative sea-level rise in the Mekong delta. *Communications Earth and Environment*, *3*(1). https://doi.org/10.1038/s43247-021-00331-3

Hung, N. N., Delgado, J. M., Güntner, A., Merz, B., Bárdossy, A., & Apel, H. (2014). Sedimentation in the floodplains of the Mekong Delta, Vietnam Part II: Deposition and erosion. *Hydrological Processes*, *28*(7), 3145–3160. https://doi.org/10.1002/hyp.9855

Kettner, A. J., & Syvitski, J. P. M. (2008). HydroTrend v.3.0: A climate-driven hydrological transport model that simulates discharge and sediment load leaving a river system. *Computers and Geosciences*, *34*(10), 1170–1183. https://doi.org/10.1016/j.cageo.2008.02.008

Kummu, M., & Koponen. (2008). Sediment: Curse or Blessing for Tonle Sap Lake? *A Journal of the Human Environment*, *37*(3), 158–163. https://doi.org/10.1579/0044

Liu, C., He, Y., Des Walling, E., & Wang, J. (2013). Changes in the sediment load of the Lancang-Mekong River over the period 1965-2003. *Science China Technological Sciences*, *56*(4), 843–852. https://doi.org/10.1007/s11431-013-5162-0

Lu, X., Kummu, M., & Oeurng, C. (2014). Reappraisal of sediment dynamics in the Lower Mekong River, Cambodia. *Earth Surface Processes and Landforms*, *39*(14), 1855–1865. https://doi.org/10.1002/esp.3573

Luu, L. X., Egashira, S., & Takebayashi, H. (2004). INVESTIGATION OF TAN CHAU REACH IN LOWER MEKONG USING FIELD DATA AND NUMERICAL SIMULATION. In *Annual Journal of Hydraulic Engineering* (Vol. 48).

Manh, N. V., Dung, N. V., Hung, N. N., Merz, B., & Apel, H. (2014). Large-scale suspended sediment transport and sediment deposition in the Mekong Delta. *Hydrology and Earth System Sciences*, *18*(8), 3033–3053. https://doi.org/10.5194/hess-18-3033-2014

Minderhoud, P. S. J., Erkens, G., Pham, V. H., Bui, V. T., Erban, L., Kooi, H., & Stouthamer, E. (2017). Impacts of 25 years of groundwater extraction on subsidence in the Mekong delta, Vietnam. *Environmental Research Letters*, *12*(6). https://doi.org/10.1088/1748-9326/aa7146

Nash, J. E., & Sutcliffe, J. V. (1970). River flow forecasting through conceptual models. Part 1: A discussion of principles. *Journal of Hydrology*, *10*, 282–290.

Romero-Díaz, A., Marín-Sanleandro, P., & Ortiz-Silla, R. (2012). Loss of soil fertility estimated from sediment trapped in check dams. South-eastern Spain. *Catena*, *99*, 42–53.

Sok, T., Oeurng, C., Kaing, V., Sauvage, S., Kondolf, G. M., & Sánchez-Pérez, J. M. (2021). Assessment of suspended sediment load variability in the Tonle Sap and Lower Mekong Rivers, Cambodia. *Catena*, *202*. https://doi.org/10.1016/j.catena.2021.105291

Sutanudjaja, E. H., Van Beek, R., Wanders, N., Wada, Y., Bosmans, J. H. C., Drost, N., Van Der Ent, R. J., De Graaf, I. E. M., Hoch, J. M., De Jong, K., Karssenberg, D., López López, P., Peßenteiner, S., Schmitz, O., Straatsma, M. W., Vannametee, E., Wisser, D., & Bierkens, M. F. P. (2018). PCR-GLOBWB 2: A 5 arcmin global hydrological and water resources model. *Geoscientific Model Development*, *11*(6), 2429–2453. https://doi.org/10.5194/gmd-11-2429-2018

Syvitski, J. P. M., & Milliman, J. D. (2007). Geology, Geography, and Humans Battle for Dominance over the Delivery of Fluvial Sediment to the Coastal Ocean. *The Journal of Geology*, *115*, 1–19.

Thorne C. R., & Osman A. M. (1988). osman-thorne-1988-riverbank-stability-analysis-ii-applications. *Journal of Hydraulic Engineering*, *114*(2), 151–172.

Van Binh, D., Kantoush, S., & Sumi, T. (2020). Changes to long-term discharge and sediment loads in the Vietnamese Mekong Delta caused by upstream dams. *Geomorphology*, *353*(107011).

Van de Wiel, M. J. (2003). *NUMERICAL MODELLING OF CHANNEL ADJUSTMENT IN ALLUVIAL MEANDERING RIVERS WITH RIPARIAN VEGETATION*.

Vörösmarty, C. J., Meybeck, M., Fekete, B., Sharma, K., Green, P., & Syvitski, J. P. M. (2003). Anthropogenic sediment retention: Major global impact from registered river impoundments. *Global and Planetary Change*, *39*(1–2), 169–190. https://doi.org/10.1016/S0921-8181(03)00023-7